REAL-TIME NONLINEAR INDIVIDUAL CYLINDER AIR FUEL RATIO OBSERVER ON A DIESEL ENGINE TEST BENCH

Jonathan Chauvin [*] **Philippe Moulin** [**]
Gilles Corde [**] **Nicolas Petit** [*] **Pierre Rouchon** [*]

[*] *Centre Automatique et Systèmes, École des Mines de Paris,*
60, bd St Michel, 75272 Paris, France
`chauvin@cas.ensmp.fr`
[**] *Institut Français du Pétrole, 1 et 4 Avenue de Bois Préau, 92852 Rueil Malmaison, France*

Abstract: We propose an estimator of the individual cylinder air fuel ratios in a turbocharged Diesel Engine using as only sensor the single air fuel ratio sensor placed downstream the turbine. The observer consists of a nonlinear filter designed on a physics-based time-varying model for the engine dynamics. Convergence is proven, using a Lyapounov function. Performance is studied through simulations and test bench experiments on a 4 cylinder engine. *Copyright* © *2005 IFAC.*

Keywords: Engine Control, Observers, Air Fuel Ratio, Individual Cylinder Observer

1. INTRODUCTION

Performance and environmental requirements impose advanced control strategies for automotive applications. In this context, controlling the combustion represents a key challenge (Guzzella and Amstutz, 1998; Kiencke and Nielsen, 2000). Several tentative solutions are combustion torque control and estimation (see for example (Guezennec and Gyan, 1999), (Chauvin *et al.*, 2004*a*) and (Chauvin *et al.*, 2004*b*)), Air Fuel Ratio control and estimation (see (Grizzle *et al.*, 1991) and (Moulin *et al.*, 2004)),.... One important step is the control of the *individual* Air Fuel Ratio (AFR) which is a good representation of the torque produced by the engine. It results from various inputs such as injected quantities and timing, exhaust gas recirculation (EGR) rate.

Classically, overall AFR can be directly controlled with the injection system (Grizzle *et al.*, 1991). In this approach, all cylinders share the same closed loop input signal based on the single AFR sensor. Ideally, all the cylinders would have the same AFR as they have the same injection setpoint. Unfortunately, due to inherent flaws of the injection system (pressure waves, mechanical tolerances, ...), the total fuel mass injected in each cylinder is very difficult to predict. Individual cylinder control has been addressed using individual cylinder AFR sensor in (Berggren and Perkovic, 1996). In practice, cost and reliability of multiple AFR sensor may prevent them from reaching commercial products lines.

For forthcoming HCCI engines (see (Kahrstedt *et al.*, 2003; Hultqvist *et al.*, 2001; Chiang and Stefanopoulou, 2004; Rausen *et al.*, 2004) for example) and regeneration filters, even slight unbalance

between the cylinders can have dramatic consequences and induce important noise, possible stall and higher emissions. Individual cylinder control is needed. In this context individual cylinder AFR estimation can give crucial information to get the HCCI running better.

The contribution of this paper is the design of a real-time observer for the individual cylinder AFR using the reliable and available AFR sensor placed downstream the turbine as only measurement.

In previous works (see (Fantini and Burq, 2003) and (Carnevale and Hadji, 1998)), the methods used to reconstruct the AFR of each cylinder from the UEGO (Universal Exhaust Gas Oxygen) sensor measurement are based on the permutation dynamics at the TDC (Top-Dead Center) sample angle and a gain identification technique. We propose here a higher frequency approach (6° sample angle instead of 90° (TDC)). We design an observer on the balance model of the exhaust and use a nonlinear observer to solve the problem. A key problem in practice is the real-time implementation on an embedded system. Compared to Kalman observers, an interesting feature of our approach is its low computational cost which makes it tractable on a typical MPC555 based embedded card system, such as found on actual test benches.

We use a physics-based model underlying the role of periodic input flows (gas flows from the cylinders into the exhaust manifold). A nonlinear observer is designed and validated both experimentally (on a four cylinder turbocharged diesel test bench presented in (Moulin *et al.*, 2004)) and theoretically (convergence is proven).

The paper is organized as follows. In Section 2, we present the exhaust modelling and the individual cylinder AFR model. In Section 3, we propose a nonlinear individual cylinder AFR observer. Simulation and experimental results are presented in Section 4. Future directions are given in Section 5.
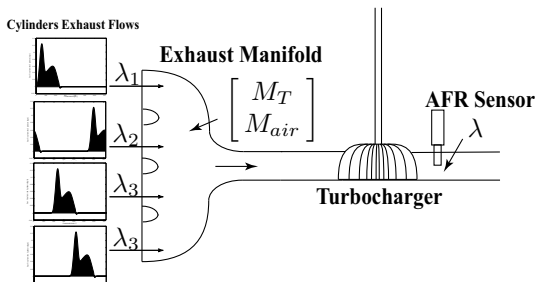
2. EXHAUST MODELLING

Figure 1. Individual Air-Fuel Ratio problem.

Figure 1 shows the flow sheet of the individual AFR from the cylinders outlet down to the turbine, where the sensor is located at. From the cylinders to the AFR sensor (located downstream the turbine) the gases travel through the exhaust pipes, the exhaust manifold and the turbocharger. All these components have an influence on the gas pressure, temperature, and composition in the exhaust manifold. In an "ideal system", the gases would move at a constant speed, without mixing. The global dynamics of the system are therefore nonlinear and depend on the operating conditions of the engine (engine speed, load, EGR). Our approach is to focus on a macroscopic balance model involving experimentally derived nonlinear functions.

2.1 Mass Balance in the exhaust manifold

Let M_T and M_{air} be the total mass of gas and the mass of fresh air in the exhaust manifold, respectively. Let λ_i be the *Air Fuel Ratio in cylinder i*. The measurements are

- P: the pressure in the exhaust manifold. This measure is not always available on a vehicle and can be given by the open loop estimate of the total mass.
- λ: the Air Fuel Ratio is equivalent to the following definition $\lambda \triangleq 1 - \frac{M_{air}}{M_T}$ with no EGR.

In the crank angle time α, on an operating point the mass balances write

$$\begin{cases} N_e \dfrac{dM_T}{d\alpha} = \sum_{i=1}^{n_{cyl}} d_i(\alpha) - d_T(M_T) \\ N_e \dfrac{dM_{air}}{d\alpha} = \sum_{i=1}^{n_{cyl}} (1-\lambda_i)d_i(\alpha) - \dfrac{M_{air}}{M_T} d_T(M_T) \\ N_e \dfrac{d\lambda_i}{d\alpha} = 0 \ \ \forall i \in [\,1, \ n_{cyl}\,] \end{cases}$$

(1)

where

- N_e is the engine speed.
- d_i is the gas mass flow from cylinder i into the exhaust manifold.
- d_T is the gas mass flow through the turbine. d_T is a function of the total mass M_T and can be factorized as $d_T(M_T) = p(M_T)M_T$ with p a function of the total mass M_T.
- n_{cyl} the number of cylinders, 4 in our case.

The d_i functions are modelled through interpolation of a large number of available data. For sake of simplicity these 4π-periodic functions are approximated using a neural network, with three inputs : engine speed, intake pressure, and crank angle. For a given operating point (engine speed, load), the flow from the cylinders are equal up to 180° shift. The mass flow through the turbine,
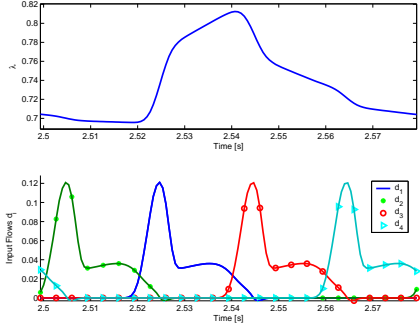
Figure 2. AFR oscillation over 1 engine cycle during a +20% offset on cylinder 1. Top: AFR. Bottom: Cylinders Input Flows.

usually given by a 2D look up table, is modelled as a flow through a restriction (Heywood, 1988) with a variable section depending on the pressure ratio and the turbocharger speed (see (Jensen *et al.*, 1991) and (Moraal and Kolmanovsky, 1999)). Moreover, corrections are made to take the turbine upstream pressure and temperature into account. The composition of the flow through the turbine is the same as in the exhaust manifold.

2.2 Reference Model

Let $x = \begin{bmatrix} M_T & M_{air} & \lambda_1 & \dots & \lambda_{n_{cyl}} \end{bmatrix}^T \in \mathbb{R}^{n_{cyl}+2}$ be the state and $y = \begin{bmatrix} P & \lambda \end{bmatrix}^T \in \mathbb{R}^2$ the measurements. System (1) rewrites as the following 4π-periodic (w.r.t. α) nonlinear model

$$\frac{dx}{d\alpha} = f(x, \alpha), \quad y = h(x) \qquad (2)$$

Where

$$f_1(x, \alpha) = \frac{1}{N_e} \left(\sum_{i=1}^{n_{cyl}} d_i(\alpha) - x_1 p(x_1) \right)$$

$$f_2(x, \alpha) = \frac{1}{N_e} \left(\sum_{i=1}^{n_{cyl}} (1 - x_{i+2}) d_i(\alpha) - x_2 p(x_1) \right)$$

$$f_i(x, \alpha) = 0 \quad \forall i \in [\, 3, \ n_{cyl} + 2 \,]$$

and

$$h_1(x) = \gamma_T x_1, \quad h_2(x) = 1 - \frac{x_2}{x_1}$$

where γ_T is a positive constant arising from the ideal gas law (temperature is assumed constant around a given operating point).

3. NONLINEAR INDIVIDUAL CYLINDER AFR OBSERVER

3.1 Observer Definition

We consider the following time-varying observer

$$\begin{cases} \dfrac{d\hat{x}_1}{d\alpha} &= f_1(\dfrac{1}{\gamma_T} y_1, \alpha) + \dfrac{L_1}{N_e}(\dfrac{y_1}{\gamma_T} - \hat{x}_1) \\[2ex] \dfrac{d\hat{x}_2}{d\alpha} &= f_2(\dfrac{1}{\gamma_T} y_1, (1 - y_2)\dfrac{1}{\gamma_T} y_1, \hat{x}_{2+i}, \alpha) \\[1ex] & \quad + \dfrac{L_2}{N_e}((1 - y_2)\dfrac{1}{\gamma_T} y_1 - \hat{x}_2) \\[2ex] \dfrac{d\hat{x}_{2+i}}{d\alpha} &= -\dfrac{L_\lambda}{N_e} d_i(\alpha)\big((1 - y_2)\dfrac{1}{\gamma_T} y_1 - \hat{x}_2\big) \end{cases} \qquad (3)$$

where the last equation hold for all i in $[\, 1, \ n_{cyl} \,]$, and where $(L_1, L_2, L_\lambda) \in (\mathbb{R}^+)^3$. To prove convergence of the observer rate $\hat{x}$, described by System (3), to the state x of the reference System (2), we exhibit a Lyapounov function and use LaSalle's theorem to conclude to the convergence of the observer.

Let $\tilde{x} = x - \hat{x}$. The error dynamics write

$$\begin{cases} \dfrac{d\tilde{x}_1}{d\alpha} &= -\dfrac{1}{N_e} L_1 \tilde{x}_1 \\[2ex] \dfrac{d\tilde{x}_2}{d\alpha} &= -\dfrac{1}{N_e} \left(\sum_{i=1}^{n_{cyl}} \tilde{\lambda}_i d_i(\alpha) + L_2 \tilde{x}_2 \right) \\[2ex] \dfrac{d\tilde{x}_{2+i}}{d\alpha} &= \dfrac{1}{N_e} L_\lambda d_i(\alpha) \tilde{x}_2, \quad \forall i \in [\, 1, \ n_{cyl} \,] \end{cases} \qquad (4)$$

3.2 Lyapounov function candidate

We consider the following Lyapounov function candidate

$$V(\tilde{x}) = \frac{N_e}{2} \left(\frac{1}{L_1} \tilde{x}_1^2 + \frac{1}{L_2} \tilde{x}_2^2 + \frac{1}{L_2 L_\lambda} \sum_{i=1}^{n_{cyl}} \tilde{x}_{2+i}^2 \right) \qquad (5)$$

On the one hand, $V(\tilde{x}) > 0$ for $\tilde{x} \in \mathbb{R}^{n_{cyl}+2} \setminus \{0\}$ and $V(0) = 0$. Then the following computation yield next lemma.

$$\begin{aligned} \frac{dV}{d\alpha}(\tilde{x}) &= -\tilde{x}_1^2 - \frac{1}{L_2} \sum_{i=1}^{n_{cyl}} \tilde{x}_{2+i} d_i(\alpha) \tilde{x}_2 - \tilde{x}_2^2 \\ & \quad + \frac{1}{L_2} \sum_{i=1}^{n_{cyl}} d_i(\alpha) \tilde{x}_2 \tilde{x}_{2+i} \\ &= -\tilde{x}_1^2 - \tilde{x}_2^2 \leq 0 \end{aligned}$$

Lemma 1. The function V defined by (5) is a Lyapounov function for the error-state System (4).

3.3 Application of LaSalle's theorem

Let $\Omega_r = \{\tilde{x}_f \in \mathbb{R}^{n_{cyl}+2} / V(\tilde{x}_f) < r\} \subset \mathbb{R}^{n_{cyl}+2}$. Ω_r is a compact set positively invariant with respect to the error dynamics because $\frac{dV}{d\alpha} \leq 0$. Therefore V is a continuously differentiable function such that $\frac{dV}{d\alpha}(\tilde{x}_f) \leq 0$ in Ω_r. Let I_f be the largest invariant set in $\{\tilde{x}_f \in \Omega_r / \frac{dV}{d\alpha}(\tilde{x}_f) = 0\}$. From LaSalle's theorem (see (Khalil, 1992) Theorem 4.4), every solution starting in Ω_r approaches I_f as $\alpha \to \infty$.

3.4 Characterization of the invariant set I_f

We first characterize $\{\tilde{x}_f \in \Omega_r / \frac{dV}{d\alpha}(\tilde{x}_f) = 0\}$ and then I_f.

$$x_0 \in \{\tilde{x}_f \in \Omega_r / \frac{dV}{d\alpha}(\tilde{x}_f) = 0\}$$
$$\Leftrightarrow -\tilde{x}_{1_f}^2 - \tilde{x}_{2_f}^2 = 0 \Leftrightarrow \begin{cases} \tilde{x}_{1_f} = 0 \\ \tilde{x}_{2_f} = 0 \end{cases}$$

Thus

$$\{\tilde{x}_f \in \Omega_r \ / \ \frac{dV}{d\alpha}(\tilde{x}_f) = 0\}$$
$$= \{\begin{bmatrix} 0 & 0 & \tilde{\lambda}_{1,0} & \dots & \tilde{\lambda}_{n_{cyl},0} \end{bmatrix}^T \in \mathbb{R}^{n_{cyl}+2}\}$$

From LaSalle's theorem, I_f is the largest invariant set in $\{\tilde{x}_f \in \Omega_r / \frac{dV}{d\alpha}(\tilde{x}_f) = 0\}$. I_f writes

$$I_f = \{\begin{bmatrix} 0 & 0 & \tilde{\lambda}_{1,0} & \dots & \tilde{\lambda}_{n_{cyl},0} \end{bmatrix}^T \in \mathbb{R}^{n_{cyl}+2} /$$
$$\forall \alpha \in [0, \ 4\pi] \ \sum_{i=1}^{n_{cyl}} \tilde{\lambda}_{i,0} d_i(\ \alpha) = 0\}$$

The functions family $\{d_i\}_{i=1\dots n_{cyl}}$ is a linearly independent family of the set $\mathcal{C}^0([0, \ 4\pi], \mathbb{R})$. Therefore the set I_f is reduced to $\{0\}$. The observation error is asymptotically stable and the following results hold.

Lemma 2. The largest set in

$$\Omega_r = \{\tilde{x}_f \in \mathbb{R}^{n_{cyl}+2} / V(\tilde{x}_f) < r\} \subset \mathbb{R}^{n_{cyl}+2}$$

invariant by the dynamics of the system (4) where the function V is defined in (5) is the null space.

Proposition 1. The observer defined in equation (3) converges toward the reference model (2).

4. SIMULATION AND EXPERIMENTAL RESULTS

4.1 Tests setup

The estimator described above is tested in simulation, on a high frequency engine model developed in AMESim (IMAGINE, 2004). This includes a complete combustion model, balance ODEs, thermal transfer laws, gas mixing laws,... On both simulation and experimental testbed, we apply an injection duration timing trajectory to introduce unbalance.It produces offsets in injection which lead to AFR disturbances. More precisely the injection steps have an effect on the average level of the measured AFR and introduce oscillations of the overall AFR signal as represented in Figure 2. These oscillations are the direct consequences of the individual AFR difference. During cylinder 1 exhaust phase, the AFR increases in the manifold, and then decreases while the other cylinders

exhaust phases occur. The magnitude of the oscillations is related to the amount of the AFR difference between the cylinders and the gas mass in the manifold (and thus to its volume). The oscillation is then propagated to the turbine, and to the UEGO sensor, where it is filtered. This is the information that we exploit in the nonlinear observer (3).
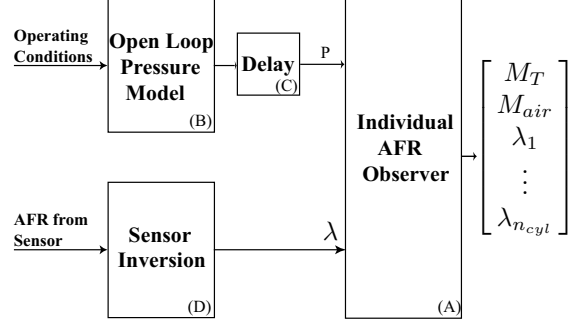

Figure 3. Observer Scheme as used in the test bench.

4.2 Simulation Results and Comments

Figure 4 presents results from simulation on the trajectory reference. The results are both quanti-
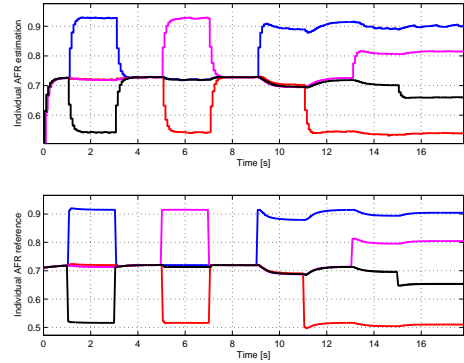

Figure 4. Trajectory on simulation at 1500 rpm and $800\mu s$ using the trajectory injection offset. Top: Reconstructed with (3). Bottom: Actual values from simulation

tatively and qualitatively accurate. We reproduce well the evolution of the AFR. In practice the convergence is achieved within 4 engine cycles. The real bottleneck is the sensor noise and the quality of its model. In our results a simple first order model was used and seems relevant for this application. Yet, as rpm increases, better approximations would be useful. These results are encouraging for control purposes.

4.3 From simulation to experimentation

On the test bench we use the proposed observer following the scheme in Figure 3. Block (A) is the

Table 1. Experimental results.

N_e	IMEP	$100\,\|\lambda_*\|_\infty$	$100\,\|\lambda_*\|_{\mathrm{mean}}$
1500	3	9.28	3.93
1500	6	3.61	1.47
1500	9	4.68	1.71
2000	6	7.29	2.27
2000	9	5.25	1.63
2500	3	7.16	3.72

implementation of observer (3). Several practical issues are considered.

Open Loop Pressure Model Depending on the vehicle, we may not have a exhaust pressure sensor. This sensor can be expected for HCCI vehicle only. In experimentation, we consider not having this sensor and give to the estimator an open loop value. This value is given by the open loop balance with the input flows (d_i) and output flow d_T as described previously in Section 2.1. This model is implemented in Block (B) in Figure 3.

Delay The lags due to the transport of the gas along the engine exhaust (pipes and volumes), and the dead time of the sensor are not represented by the model described above in System (2). However, all the delayed values used the same delay, the delays can be lumped in a single delay for the complete exhaust system, and the model can be inverted as it is. The global delay can be identified inline on the first offset. This estimated value is then kept as a constant for a given setpoint on the (engine speed, load) map. This estimation is implemented in Block (C) in Figure 3.

AFR Sensor Inversion The AFR sensor has a low-pass transfer function. Quantification noise is filtered by a very high frequency low-pass filter. The dynamics can be approximated by a first order filter. In order to robustly invert this dynamics, we apply an observer based on an adaptive Fourier Decomposition (Block (D) in Figure 3).

4.4 Experimental Results and Comments

We applied the same injection duration timing trajectories at the test bench. The test bench used for validation is a 4 cylinders DI engine with a Variable Geometry Turbocharger (VGT) (see (Moulin *et al.*, 2004)). We can see the results in Figures 5 and 6. These represent the nonlinear estimation of the individual cylinder AFR around two engine setpoints. The same parameters were kept from simulation to experimentation.
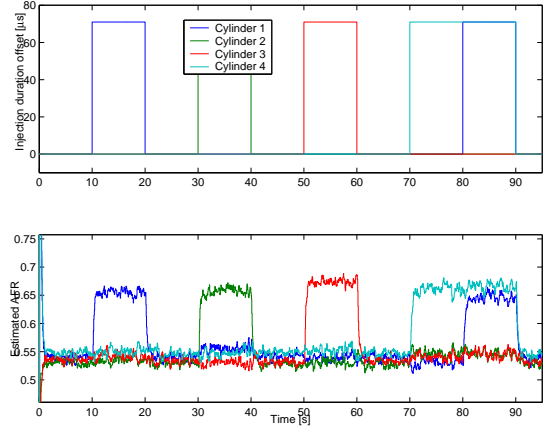

Figure 5. Test bench (2000 rpm and 6 bar). Top: Injection Duration Offsets. Bottom: Individual Estimated AFR
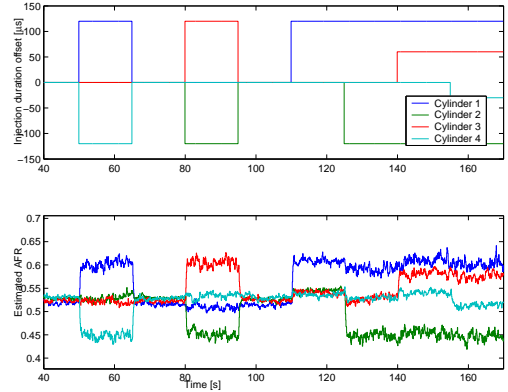

Figure 6. Test bench (1500 rpm and 6 bar). Top: Injection Duration Offsets. Bottom: Individual Estimated AFR

Further tests were conducted. Numerical values are reported in Table 1. They quantify the results of our observer for several setpoints (Engine Speed (rpm), IMEP (bar)). The reference AFR are not directly available but we can correlate them to the torque produced by each cylinder (reconstructed from the experimental individual in-cylinder pressure sensors). These correlated values, noted λ_{ref}, serve as a reference for the AFR in each cylinder. For this study we define two norms which represent (around steady states) the maximum and the mean value of the relative absolute errors around steady state.

- $\|\lambda_*\|_\infty \triangleq \max_{i,\alpha} \left| \frac{\hat{\lambda}_i - \lambda_{i,ref}}{\lambda_{i,ref}} \right|$
- $\|\lambda_*\|_{\mathrm{mean}} \triangleq \mathrm{mean}_{i,\alpha} \left| \frac{\hat{\lambda}_i - \lambda_{i,ref}}{\lambda_{i,ref}} \right|$

In all test bench cases, we were able to predict the individual cylinder AFR well. Further, we can easily detect the AFR unbalance and have a good estimation of the peaks of the AFR disturbances, the magnitude of the individual AFR offsets are satisfactory.

5. CONCLUSIONS AND FUTURE DIRECTIONS

The work presented in this paper reports the development and implementation of a individual cylinder AFR estimator. It reconstructs the AFR of each cylinder from a measurement made by a *single* sensor located downstream the turbine. The availability of such an estimator giving reliable information can lead to improvements on diesel engines in terms of combustion control, noise, and pollutant emissions. This information will be used to control the unbalance between the cylinders. Indeed by controlling the individual injection quantity (which is the relevant control for such unbalance observation) a simple PI controller will lead to the balance of the individual AFR. In the context of combustion real-time control, this observer is a handy tool. It could be used in a closed loop controller of the fuel injectors. This is the long term goal of our work. Moreover this observer is easily transposed to various engine speeds and loads. Its dynamics are expressed in angular time scale and do not require any model for the combustion process. Theoretically, the gains do not need to be updated when the setpoint is changed. However we need to integrate the exhaust gas recirculation flow (EGR) for the HCCI purpose. We are currently investigating this point in an exhaustive test campaign on the test bench.

REFERENCES

Berggren, P. and A. Perkovic (1996). Cylinder individual lambda feedback control in an SI engine. Master's thesis. Linköpings Universitet.

Carnevale, C. and M. Hadji (1998). Cylinder to cylinder AFR control with an asymmetrical exhaust manifold in a GDI system. In: *Proc. of SAE Conference.* number 981064.

Chauvin, J., G. Corde, P. Moulin, M. Castagné, N. Petit and P. Rouchon (2004a). Real-time combustion torque estimation on a Diesel engine test bench using an adaptive Fourier basis decomposition. In: *IEEE Proc. of 2004 Conference in Decision and Control.*

Chauvin, J., G. Corde, P. Moulin, M. Castagné, N. Petit and P. Rouchon (2004b). Real-time combustion torque estimation on a Diesel engine test bench using time-varying Kalman filtering. In: *IEEE Proc. of 2004 Conference in Decision and Control.*

Chiang, C.J. and A.G. Stefanopoulou (2004). Steady-state multiplicity and stability of thermal equilibria in Homogeneous Charge Compression Ignition (HCCI) engines. In: *IEEE Proc. of 2004 Conference in Decision and Control.*

Fantini, J. and J.F. Burq (2003). Exhaust-intake manifold model for estimation of individual cylinder air fuel ratio and diagnostic of sensor-injector. In: *Proc. of SAE Conference.* number 2003-01-1059.

Grizzle, J., K. Dobbins and J. Cook (1991). Individual cylinder air-fuel ratio control with a single EGO sensor. *Proc. in the IEEE Transactions on Vehicular Technology* **40**(1), 357–381.

Guezennec, Y. and P. Gyan (1999). A novel approach to real-time estimation of the individual cylinder pressure for S.I. engine control. In: *Proc. of SAE Conference.*

Guzzella, L. and A. Amstutz (1998). Control of Diesel engines. *Proc. in the IEEE Control Systems Magazine* **18**, 53–71.

Heywood, J.B. (1988). *Internal Combustion Engine Fundamentals.* McGraw-Hill, Inc.

Hultqvist, A., U. Engdar, B. Johansson and J. Klingmann (2001). Reacting boundary layers in a homogeneous charge compression ignition (HCCI) engine. In: *Proc. of SAE Conference.* number 2001-01-1032.

IMAGINE (2004). *AMESim user manual, http://www.amesim.com/.*

Jensen, J.P., A.F. Kristensen, S.C. Sorensen, N. Houbak and E. Hendricks (1991). Mean value modeling of a small turbocharged diesel engine. In: *Proc. of SAE Conference.* number 910070.

Kahrstedt, J., K. Behnk, A. Sommer and T. Wormbs (2003). Combustion processes to meet future emission standards. In: *MTZ.* pp. 1417–1423.

Khalil, H.K. (1992). *Nonlinear Systems.* Prentice-Hall, Inc.

Kiencke, U. and L. Nielsen (2000). *Automotive Control Systems For Engine, Driveline, and Vehicle.* SAE Internationnal.

Moraal, P. and I. Kolmanovsky (1999). Turbocharger modeling for automotive control applications. In: *Proc. of SAE Conference.* number 1999-01-0908.

Moulin, P., G. Corde, J. Chauvin and M. Castagné (2004). Cylinder individual AFR estimation based on a physical model and using kalman filters. In: *Proc. of the FISITA World Automotive Congress 2004.* number F2004V279.

Rausen, D.J., A.G. Stefanopoulou, J-M. Kang, J.A. Eng and T-W. Kuo (2004). A mean-value model for control of Homogeneous Charge Compression Ignition (HCCI) engines. In: *IEEE Proc. of 2004 American Control Conference.*